Crossing the Reality Gap in Tactile-Based Learning

Ya-Yen Tsai[1], Bidan Huang[2†], Yu Zheng[2], Lei Han[2], Wang Wei Lee[2], Edward Johns[1]

***Abstract*— Tactile sensors are believed to be essential in robotic manipulation, and prior works often rely on experts to reason the sensor feedback and design a controller. With the recent advancement in data-driven approaches, complicated manipulation can be realised, but an accurate and efficient tactile simulation is necessary for policy training. To this end, we present an approach to model a commonly used pressure sensor array in simulation and to train a tactile-based manipulation policy with sim-to-real transfer in mind. Each taxel in our model is represented as a mass-spring-damper system, in which the parameters are iteratively identified as plausible ranges. This allows a policy to be trained with domain randomisation which improves its robustness to different environments. Then, we introduce encoders to further align the critical tactile features in a latent space. Finally, our experiments answer questions on tactile-based manipulation, tactile modelling and sim-to-real performance.**

I. INTRODUCTION

Tactile feedback is indispensable for humans in object manipulation. It complements the vision by providing direct sensing at the point of contact or when a line of sight is occluded by hands. Tactile can provide information such as contact forces and locations, allowing humans to infer the physical properties of the handling object and maneuver it with fine control [1], [2]. Inspired by human touch feedback, many tactile sensors have thus been integrated into robotic hands with the aim of achieving human-like sensing and manipulation ability. Examples include DLR-HIT hand [3], Schunk Dexterous Hand [4] and iCub [5]. A large number of these sensors are sensor arrays that consist of multiple sensor units, i.e. taxels, converting the pressure to electrical signal. The compact form factor and high response rate make them ideal for serving as robot skin or for manipulations with fast control rate.

Recently, data-driven approaches have gained much popularity in learning robotic manipulations. They scale well in interpreting unstructured and high-dimensional features and learning complex policies compared to hand-crafted approaches. These approaches often rely on simulations to provide efficient ways for large data collection and strategies like domain randomization to cross the reality gap. For tactile-based robotic manipulation, most tactile simulations leveraged models based on finite element methods or tactile image reconstruction [6]–[8]. While they allow delicate simulation of the deformation or response of tactile sensors, they are not originally proposed to cater for tactile-based learning and with sim-to-real transfer in mind. Learning tactile-based manipulation with these simulations will hence be expansive and less ideal.

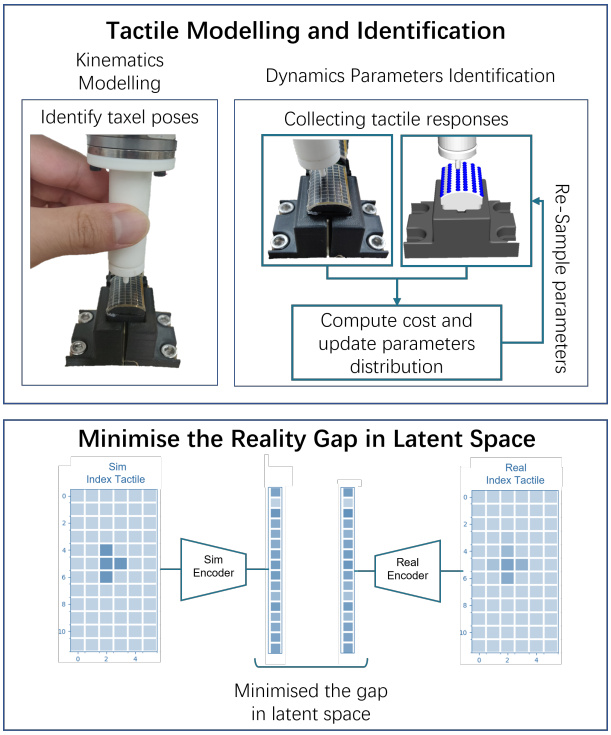

Fig. 1: An overview of tactile simulation and sim-to-real strategy to close the reality gap of the tactile signals in the latent space.

To this end, we propose a novel framework that achieves a good balance between accuracy and speed in tactile simulation and focuses on crossing the reality gap in tactile-based learning. In particular, we study the pressure sensor arrays and model each taxel as a mass-spring-damper system. By conducting the same experiments in the simulation and the real environment, the kinematics and dynamics of the tactile sensors are calibrated. Different from most approaches, we take the real sensor noise into account and calibrate the parameters of each taxel by probabilistic distributions rather than using deterministic values. The distributions serve as domain randomization ranges of the environment where a policy is trained, thus improving the robustness of the policy in sim-to-real transfer. Above all, we admit the fact that even with careful calibration, the raw simulation tactile signal cannot perfectly replicate the real one, and we align the

† indicates the corresponding author.
[1]Y.-Y. Tsai and E. Johns are with the Department of Computing, Imperial College London, SW7 2AZ, London, UK (e-mail: {y.tsai17, e.johns}@imperial.ac.uk).
[2]B. Huang†, Y. Zheng, L. Han, and W.W. Lee are with Tecent Robotics X, Shenzhen, China (e-mail: {bidanhuang, petezheng, lxhan, wwlee}@tencent.com).

simulation and real tactile signal in a latent space. A pair of encoders are trained to extract only the critical tactile information and the reality gap of the tactile model is minimized by the encoded signal.

We verify the proposed approach through a grasping experiment and the results have shown that the simulation-learned policy can be transferred to reality without further training and with high success rates across unseen objects. With the experiments, we try to answer the following questions regarding tactile-based manipulation and sim-to-real transfer. 1) What is the performance of the simulated tactile model? 2) Is this tactile simulation good enough for robot learning? 3) What is an effective approach to cross the tactile sim-to-real gap?

To summarise, our contribution is as follows

- An efficient, accurate, and easy-to-implement tactile sensor simulation model allowing large-scale data collection for policy learning is presented.
- A full solution of sim-to-real transfer for tactile-based learning is proposed.
- Experiment validation of the proposed tactile model and sim-to-real solution with multiple ablation studies is reported.

II. Related Work

A. Tactile Sensors

Tactile sensors have been developed for robotic manipulation to achieve human-level dexterity. Different sensing mechanisms have been proposed and the basic principle is to capture the sensor deformation caused by contact force. A large number of tactile sensors capture the deformation by electric signals, such as capacitive sensors [9], [10], and resistive sensors [11], [12]. These sensors are in the form of sensor arrays. A fluid-based sensor like BioTac [13] applies incompressible conductive fluid to change the impedance and, thus, the signals during contact. Recently, optics-based sensors have been proposed to capture the sensor surface deformation by camera [14]–[16]. In this work, we consider pressure sensor arrays due to their wide availability and use in robotic hands.

B. Tactile Simulation

Simulation provides a safe and efficient data collection approach and is generally used in robotics as an alternative to real-world data collection. To this end, several tactile simulation methods have been proposed recently, including Finite Element Methods (FEM) and image-based methods. FEM approaches model the deformation of a tactile sensor by first dividing the sensor into smaller elements and then calculating the force propagation among them [7], [17]–[19]. This can simulate complex interactions between the environment and the sensor and the deformation of the sensor to the neighbouring from the point of contact.

Image-based approaches, on the other hand, aim to simulate the real image captured by the camera. To model the deformation of the soft membrane on the sensor surface, Gomes et al. used a smoothed depth image of the contact surface [8]. Si et al. applied gelpad FEM model to model the membrane [20]. Computer graphic techniques are used to render the tactile image, such as ray tracing [21], and the shadow and the illustration of light are simulated. The generated tactile images can be used for grasp stability prediction [21], [22] and pose estimation [23] and the image fidelity is visually judged.

Mesh is another popular tactile model for studying how the contact force propagation from the point of contact to its neighborhood [24], [25]. For example, Kappassov et al. [26] simulate the deformation based on a point spread function empirically defined. Ding et al. [27], on the other hand, define the force propagation from the point of contact using a set of pushing and pulling forces.

Many of these tactile sensor simulations are designed to accurately model the deformation of tactile sensors but are not originally designed for robot learning. Their performances in learning and sim-to-real have not been optimized and fully examined.

C. Tactile Sim-to-Real

Robot learning from simulation often faces the problem of the reality gap. The differences in data distribution between the simulation and reality can result in simulation-learned policy failing in reality. To address the gap present in the FEM model of the BioTac sensor [28], Narang et al. trained a mapping between the deformation in simulation to the electrical signal in reality. For image-based tactile simulation, [29]–[31] proposed to close the gap by processing the real tactile images to match the simulated ones. Leveraging domain randomisation technique and training a policy in different environments have been shown to improve the sim-to-real transfer of tactile-based policy [12], [27].

In this work, we reconsider tactile modeling and propose a framework to tackle the sim-to-real problem in tactile-based learning. Our approach adopts a similar mass-spring-damper model used in SkinSim [32] to emulate the deformation behaviour of the robot skin. SkinSim model consists of a skin and a sensor layer, in which multiple skin units, each represented by a mass-spring-damper model, correspond to one sensor unit. In comparison, our model uses a single mass-spring-damper system to represent one taxel. This approximated model is used in exchange for improved simulation speed and its reality gap is crossed in two steps. In the first step, the parameters of the tactile model are identified as distributions, allowing domain randomization to be applied during policy training. In the second step, we address the sim-to-real gap in the latent space via tactile embedding. Experiment results have shown that this approximated model is efficient in grasp learning.

The rest of the paper is organized as follows. In Sec. III, the tactile sensor and its modeling in simulation are first presented. Then, we detail how we further bridge the reality gap in the tactile embedding. Sec. IV present the experiments used to verify the proposed approach and answers to the questions in learning tactile-based manipulation and sim-to-real transfer. Finally, we conclude our work in Sec. V

III. METHODOLOGY

In this section, we detail our tactile model and the sim-to-real strategy. After describing the physical tactile sensor (Sec. III-A), we explain the modeling and calibration principle (Sec. III-B). The alignment of the simulated and real tactile signals is achieved by kinematics and dynamic calibration. Then, the interpretation of tactile signals and policy are learned via reinforcement learning in simulation. Finally, we project both the real and the simulated tactile information to a latent space and to further cross the sim-to-real gap (Sec. III-C).

A. Tactile Sensor

Our work considers a multi-fingered robotic hand covered with an in-house piezoresistive tactile sensor. This in-house sensor is a pressure sensor array and shares the same advantages as others by offering a compact form factor, high response rate, and high temporal resolution. It can be placed on the surface of the hand and integrated into policy with fast control rate. There are 12x6 independent sensing units or taxels on the sensor, and these taxels are arranged in an array form. Each unit is a piezoresistive element, which response to an external force by changing its resistance. The sampling rate of the sensor is 200 Hz. Each sample consists of 72 tactile signals, the measurements of the current passing through piezoresistive elements.

The fingertip of the robotic hand has three layers, from top to bottom, a taxel, a curved and hollow rubber pad and a rigid tactile fixture. The sensor sits on the deformable rubber pad, which acts as a support and helps maximise the contact area during grasping. The pad is then placed on the rigid tactile fixture, which connects to a finger of the robotic hand.

B. Tactile Sensor Modelling in Simulation

Our tactile model is developed in an open source physics engine Mujoco[1], which is commonly used in robotics and machine learning community. It is chosen because it can provide a good approximation of the real contact dynamics and efficient data collection for reinforcement learning. The deformation of the tactile sensor is simulated by a group of mass-spring-damper attached to the robot hand. When the robot touches an object, the virtual springs at the contact area compress accordingly and hence produce a deformed contact surface. By optimizing the parameters of each mass-spring-damper, we can approximate the physical response of the rubber pad at contact, hence simulate the digital response of the tactile sensor. The implementation of this model is detailed in the following paragraphs.

In the simulation, the rubber pad and the tactile fixture are both rigid bodies and are built from CAD (Fig. 2). Taxels are fixed to the tactile fixture. Each taxel consists of two rigid bodies, a hemispherical mass, and a rectangular taxel base, as shown in Fig. 2(b). The mass is connected to the base via a sliding joint acting as a virtual spring. This joint limits the mass to move in one dimension, in this case, perpendicular to the curved surface of the pad. The mass is modelled in a hemispherical shape to allow objects to move smoothly along the sensor surface without getting stuck in between the taxels. A touch sensor element is placed on the top of the taxel base. This defines an active zone where collisions between bodies can be sensed. This sensor element outputs the sum of normal forces from all included contacts, i.e. the hemisphere and the base. Note that in this model each taxel is an independent sensing unit, and the force propagation between the adjacent taxels is neglected. This is due to the fact that the rubber pad in our sensor is relatively stiff and the crosstalk between the taxels does not make a major contribution to the tactile readings. This model can be considered a simplified FEM with a minimum level of complexity.

A kinematic calibration and a dynamic identification are required to align the tactile sensor in the simulation and the reality. The former measures the pose of each taxel in the coordinate frame of the tactile fixture, while the latter optimizes the dynamic parameters of each taxel such that the simulated tactile readings replicate the real one. Given the pose of each taxel from the kinematic calibration, dynamic calibration is conducted by performing the same indentation actions in both reality and simulation. By comparing the responses of the simulation against reality, we infer the possible ranges of the values of the dynamic parameters (Fig. 1). This is an essential step towards bridging the sim-to-real gap. In the following sections, these two calibrations are described in more details.

a) Kinematics Calibration: This step is to determine the pose of each taxel taking into account the misalignment of the sensor and fixture during assembly. To measure the pose in reality, we construct a calibration platform, as shown in Fig. 2(a), and use a 7 dof robotic arm as a measuring tool. In this setup, a 3D-printed indentor is fixed on the robot's end-effector, while the tactile fixture is secured by its holder. Both the robot arm and the holder are placed on an optical table.

The pose of a taxel is measured by manually dragging the tip of the indentor to touch the 4 taxels at each corner and recording the robot's pose relative to its base frame (Fig. 2(d)). As our fingertip is curved, we also touch the 3rd taxels at the top and bottom row to calibrate the curvature.

Given the CAD models of the indentor, tactile fixture and holder and the relative pose between the robot base and tactile holder can be explicitly measured using the optical table, and we can then compute the relative poses of the six touched taxels to the tactile fixture. To minimise the potential errors that arise from measurements, this step is repeated multiple times. With these 6 poses, all the other taxels' poses are computed by interpolation. Once we have obtained the poses of all taxels, a corresponding kinematic modeling of the tactile sensor can be constructed in simulation, and so does the calibration setup used for indentation (Fig. 2(a)).

b) Dynamics Identification: Dynamics identification is performed to identify the dynamics parameters of the mass-spring-damper system of each taxel, so it correctly describes the deformation behavior of the rubber pad. This behavior

[1]https://mujoco.org/

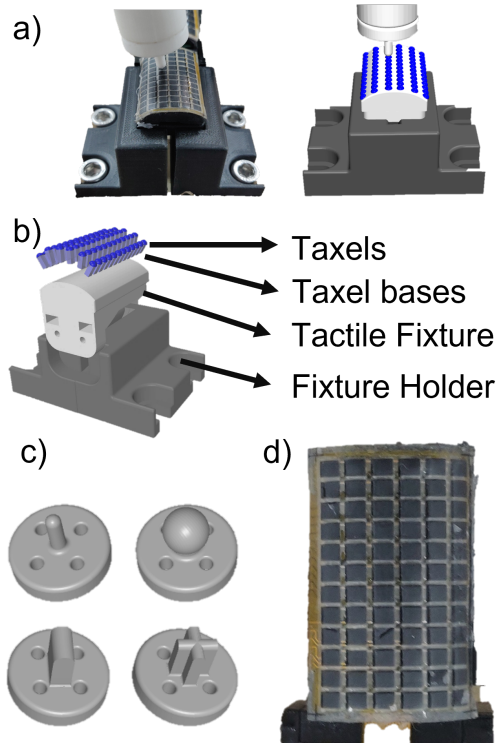

Fig. 2: a) Comparison of tactile calibration setup in simulation and reality b) Tactile sensor model in simulation c) 4 different shapes of indentors used to calibrate the sensors in simulation and reality. The shapes include small sphere, large sphere, flathead and cross. (d) A real tactile sensor which consists of 12-by-6 tactile elements arranged in the array form.

then affects the force applied to the taxel, and hence affecting its output signal. For each taxel, four parameters that affect the dynamic responses are identified. These parameters are the mass of a taxel, stiffness coefficient, damping coefficient and the distance between the taxel and taxel base along the sliding direction.

However, correctly modelling the behaviour of the tactile sensor is difficult. First, the responses of the tactile sensor are often time-variant. They could be affected by factors like materials, temperatures, and potential crosstalk etc, resulting in inconsistent responses even under the same external force. Furthermore, the signals of the sensor may fluctuate even when a constant force is applied, preventing us from accurately observing the true signals. Lastly, since as our simulation model is simplified, it may be difficult to identify the precise values for the associated dynamics parameters. Therefore, we propose to identify the distributions of dynamics parameters for each taxel. And, a policy could later be trained on environments sampled from these distributions, to increase its robustness in different environments. A stochastic and gradient-free approach - Covariance Matrix Adaptation Evolution Strategy (CMAES) [33] is used to identify the distributions for each taxel.

Given the calibration setup in reality from the last step and the identified pose of each taxel, a robot trajectory is planned to bring the indentor of Frank robot to press a taxel by 1mm and then release it. Multiple indentations are carried out, and the taxel responses during the indentations are recorded. The responses are time-indexed and normalised using the maximum values. This set of normalised time-indexed responses are denoted $\mathbf{S_{real}}$. To then identify the distributions of dynamics parameters in simulation, we first construct a simulation with the identical calibration setup to the reality, but with MuJoCo's default dynamics parameters. To apply CMAES for dynamics identification, an initial parameter distributions $\Theta_{init} = \mathcal{N}(\boldsymbol{\mu}_{init}, \boldsymbol{\Sigma}_{init})$ is guessed. At each iteration, M sets of different parameter combinations are sampled from the current distribution, θ. Each set of combinations modifies the dynamics parameters of a taxel in the calibration setup of simulation. The planned trajectory are repeatedly carried out in simulation to indent the taxel, of which the time-indexed responses are recoreded. The recorded responses are also normalised using the maximum values and are denoted $\mathbf{S_{sim}}$. We define a cost function ($\mathcal{C}$) to compare each set of $\mathbf{S_{sim}}$ against $\mathbf{S_{real}}$ and calculate the cost associated to each set of parameter combinations. The function is defined as follows:

$$\begin{aligned}\mathcal{C} =& w_1 \cdot \sum_{t=0}^{T_c} \|S_{sim,t} - S_{real,t}\| + \\ & w_2 \cdot \sum_{n=0}^{N} 1(p_n > p^n_{max}) \cdot \exp(2p^n / p^n_{max})\end{aligned} \tag{1}$$

where w_i is the weight associated with each cost term, t is the index of time, T_c is the contact duration, p^n is the n-th dynamics parameter, and p^n_{max} is the upper limit for the n-th parameter. The last term of the cost function is penalise CMAES from sampling values outside the valid ranges.

Given the k best-scored parameter combinations, the CMAES then updates the parameter distributions θ and the hyper-parameters. In the next iteration, new sets of parameter combinations are sampled from the updated distributions and the same process is iterated until convergence or a maximum defined iteration is reached. At the end of the iteration, $\Theta^* = \mathcal{N}(\boldsymbol{\mu}^*, \boldsymbol{\Sigma}^*)$ is determined and used as ranges for domain randomisation for the taxel during policy training. This dynamics calibration process is repeatedly carried out for every taxel and the calibrated tactile sensor model consists of a total of 72 sets of Θ^*.

C. Learning The Tactile Embedding

After the kinematic and dynamic calibration, the difference between the raw real and simulated tactile signal is minimized but not eliminated (Fig. 3). In this tactile embedding step, the reality gap is further reduced in a latent space. To this end, two tactile encoders are introduced in our framework: the simulation encoder referred to as the sim encoder in the rest of the article, and the real encoder. These encoders take different roles: the sim encoder extracts the critical tactile features from the raw data and reduces the

dimension of signals for fast policy learning, and the real encoder minimizes the reality gap (Fig. 1).

The sim encoder follows the standard structure of an autoencoder, which encodes the raw tactile signals in simulation into a latent representation. The autoencoder is trained to encode and reconstruct the same tactile signal at an instance of time, and its loss function follows a standard L2 norm. It is trained in concurrent with the policy training, and the training data comes from the tactile signals collected from exploratory training.

The real encoder, on the other hand, encodes the real tactile signal, into the same latent space as the previous encoder. It also has the same network structure as the first encoder, but is trained in a supervised learning fashion. The training of the second encoder is done after policy learning and after the first encoder is trained. The training data is collected using the previous calibration setup and the planned indentation trajectory. A pair of $\mathbf{S}_{\mathbf{sim}}^{\mathbf{train}}$ and $\mathbf{S}_{\mathbf{real}}^{\mathbf{train}}$ is the tactile signals collected by indenting each taxel with different types of indentors in Fig. 2(c) in both simulation and reality. The responses from different indentors are included to emulate different shapes of contact during grasping. To train the second encoder to encode $\mathbf{S}_{\mathbf{real}}$ into the same latent space as the first one, we obtained $\mathbf{S}_{\mathbf{sim}}^{\mathbf{enc}}$ by providing $\mathbf{S}_{\mathbf{sim}}^{\mathbf{train}}$ to the first encoder and use it as the ground truth. Then, the corresponding $\mathbf{S}_{\mathbf{real}}^{\mathbf{train}}$ is given to the second encoder, which is trained to minimize its output response and the corresponding $\mathbf{S}_{\mathbf{sim}}^{\mathbf{enc}}$ using the L2 norm loss function.

IV. Experiments And Results

We conducted two experiments to examine the tactile model in simulation and the reality gap of the model. These experiments were designed to answer the questions listed in the introduction (Sec. I).

A. What is the performance of the simulated tactile model?

To evaluate the tactile sensor model, we compared its tactile response against the response of the real sensor under various indentations. Both the raw tactile signals and the embedding of the signals were examined. Fig. 4 compares the raw tactile responses when both the simulated and real tactile sensors were indented by the small sphere indentor. The green, blue and orange lines indicate the real tactile signals, simulated tactile signals before and after calibration. From the figure, the calibrated tactile sensor clearly followed better the real tactile sensors in terms of the time-indexed values and contact duration compared to the uncalibrated tactile sensor. We then examined the tactile responses under different indentations. Fig. 3 shows the indented patterns and the corresponding patterns in the latent space when the tactile sensor was pressed by the indentors of a small sphere, large sphere, flathead and cross. Results have shown that the indented patterns on a tactile sensor were similar, but slight differences can be noted in the tactile intensity even after calibration. Besides each 12-by-6 matrix is a 16-by-1 matrix that shows the corresponding tactile patterns in the latent space. The tactile patterns came from the outputs of the two encoders, in which the first encoder encodes the raw signals of the simulated tactile sensor and the second encodes the raw signals of the real tactile sensor. With the help of encoders, we can clearly see that in the latent space, the tactile patterns from simulation and reality matched very well. This implies the feasibility of using encoders to further cross the sim-to-real gap in the tactile signals.

B. Is this tactile simulation good enough for robot learning?

A robotic grasping task was carried out to evaluate the simulated tactile sensor model. The robot was trained to perform a precision grasp, in which only the fingertips were allowed to grasp and pick up an unknown object from a table as illustrated in Fig. 5(b). This task is chosen as a precision grasp requires a precise relative pose between the object and fingers and sufficient contact force to pick up the object without dropping, for which tactile sensors can provide useful information. Compared to a power grasp, a precision grasp leaves flexibility for a robot to then carry out downstream manipulation.

The robot used was a 7 DoF Frank robot attached with an Allegro robotic hand at its end-effector. The hand has 4 fingers, each of which has 4 DoF. The fingertips of the Allegro hand were replaced with tactile fixtures and tactile sensors. Only the thumb and index fingers were served for precision grasp and picking.

To train the robot, we adopted an expert-student learning framework to accelerate the learning of the student policy. A model predictive controller was implemented as the expert policy. At each step, it selects an optimal action given the state and defined cost function. A Twin Delayed DDPG (TD3) was the student policy, which first learned from the expert and then improved its policy through self-exploratory training. It was trained to take the historical observations of the environment and output the Cartesian velocity of the end-effector and joint velocity of the fingers. Four objects on left of Fig.5(a) were used during training. At test time, only the student policy was deployed for the grasping tasks. Six objects unseen to the robot on Fig.5(b) were used for evaluation in simulation. The corresponding objects in Fig.5(c) were used for evaluation in reality. At training and testing, we randomised the initial position of an object inside the workspace of the hand. We assumed vision was used in prior to grasping and the estimation error was up to 2cm. At test time, each object was evaluated for 50 and 20 times in simulation and reality.

We implemented the proposed approach and additional 5 baselines for comparisons. They differed in the tactile model, and representation used during training, and strategy to cross the reality gap.

a) Proposed approach: The policy of the proposed approach took the historical observation of end-effector pose, finger joint positions, encoded tactile signals and pose of an object before grasping began. The raw tactile signal was generated from the calibrated tactile model, i.e. $\boldsymbol{\mu}^*$, and then encoded as described in Sec. III-C. To cross the reality gap,

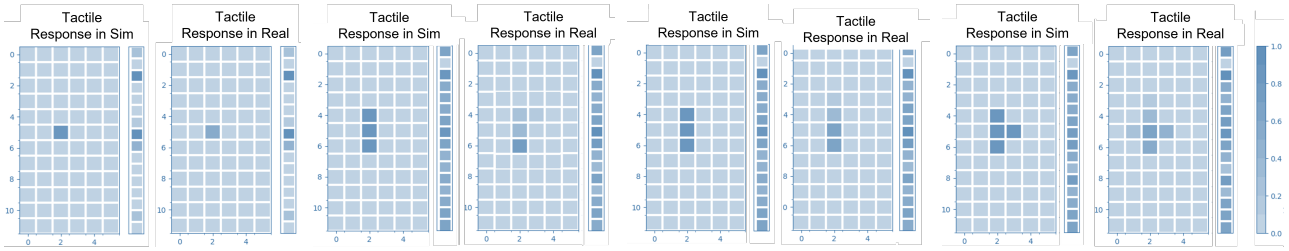

(a) (b) (c) (d)

Fig. 3: Comparison of tactile responses between simulation and reality when pressed by the same indentor. Each subplot has a 12-by-6 matrix, which shows the responses of a sensor, and has a 16-by-1 matrix which shows the corresponding latent response. The colour bar On the right-hand side shows the intensity of the response. Four shapes of indentors are evaluated. (a) small sphere (b) large sphere (c) flathead (d) cross.

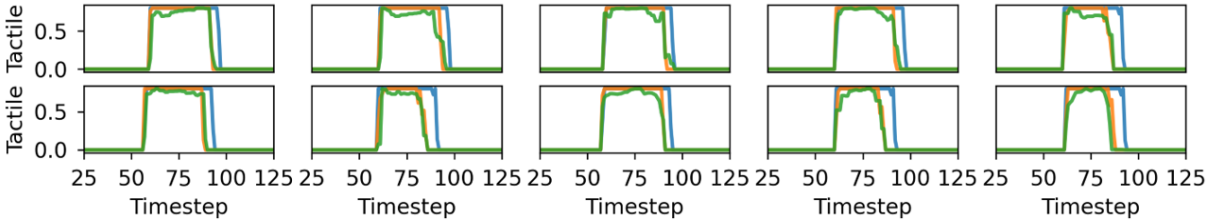

Fig. 4: Comparison of normalised and raw taxel signals from simulation and reality. Each subplot compares the responses of a taxel under the identical indentation action from simulation and reality. The green, blue and orange lines represent the real tactile signals, the simulated signals before calibration and the simulated signals after calibration. The vertical and horizontal axes are the signal intensity and the timestep.

the domain randomisation technique was applied with the randomised ranges being the estimated $\boldsymbol{\Sigma}^*$.

b) Baseline 1: Baseline1 was implemented to take the same historical observation as the proposed approach but without tactile feedback.

c) Baseline 2: Baseline2 was implemented to use the raw tactile signals generated from a hand-calibrated tactile model, i.e. $\boldsymbol{\mu}_{init}$. The manually defined domain randomisation ranges, $\boldsymbol{\Sigma}_{init}$ was used during training.

d) Baseline 3: Baseline3 was implemented to use the raw tactile signals generated from the calibrated tactile model, i.e. $\boldsymbol{\mu}*$, but domain randomisation was not applied during training.

e) Baseline 4: Baseline4 was implemented to use the encoded tactile signals in its observation. During training, the raw tactile signals were generated from a hand-calibrated tactile model, i.e. $\boldsymbol{\mu}_{init}$, and were encoded by $\hat{S_{sim}}$. At test time, the raw tactile signals from the sensor were also encoded by the same encoder. Domain randomisation was applied to randomised the dynamics parameters of all taxels within $\boldsymbol{\Sigma}_{init}$.

f) Baseline 5: Baseline5 was also implemented to take the encoded tactile signals in its observation but used the calibrated tactile model, i.e. $\boldsymbol{\mu}^*$, during training. The raw tactile signals from simulation and reality were both encoded by the same encoder, $\hat{S_{sim}}$. Domain randomisation was not applied during training.

C. *Is tactile feedback essential in tasks like precision grasp?*

The performance comparison between different grasping policies is shown in Fig. 6. From our experiment, we found out that at testing, Baseline1 did not perform further exploration to correct the pose estimation error. Instead, it almost always performed the same grasping actions regardless of the initial position of an unknown object. As such, the workspace in which the hand can successfully grasp an object was limited. This finding coincides with the results in Fig. 6. We see that the policy achieved higher success rates for objects of larger sizes but failed mainly in the smaller objects like triangular and cross prisms. For the proposed approach, while similar success rates were observed for larger objects, the tactile-based policy showed better performance for smaller objects. This result was in line with our expectations that the tactile can be helpful in precision grasp.

However, representations of tactile feedback did not seem to have much impact on the success rate of grasping. This can be seen if we compare the performance of Baseline2 to Baseline4 and Baseline3 to Baseline5. By comparing the success rates from simulation, using raw tactile signals in the observation as in Baseline2 and Baseline3 did not appear disadvantageous to using the encoded signals as in Baseline4 and Baseline5. Without explicitly encoding the raw signals, we suspect that Baseline2 and Baseline3 may have learned to perform similar encoding in their policies.

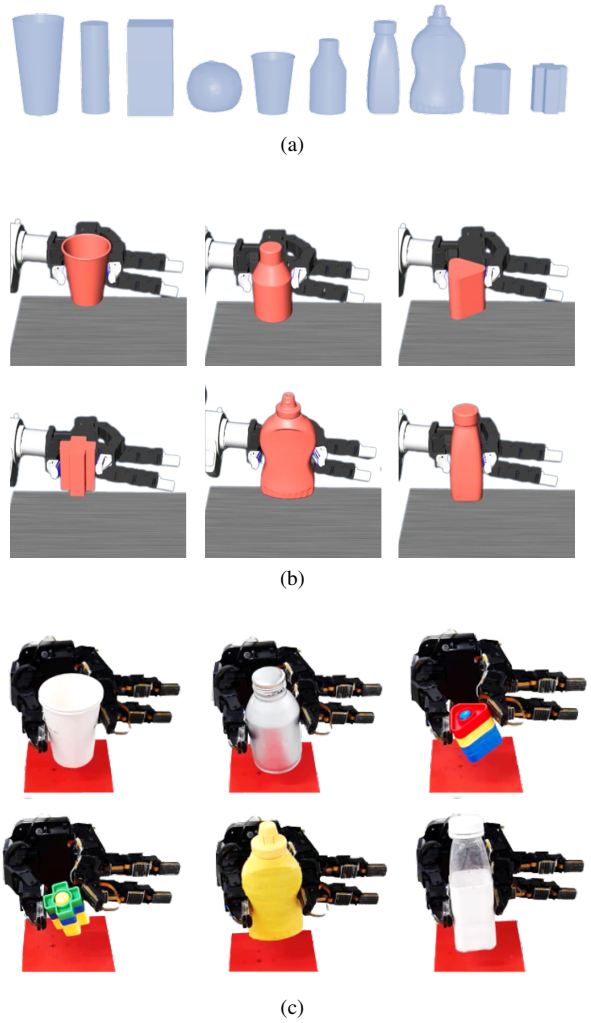

Fig. 5: (a) The first four objects are used for training and the others are for testing (b) shows the objects used for testing and the grasping results of the proposed approach in simulation. (c) shows corresponding objects used for testing and the grasping results of the proposed approach in reality.

D. What is an effective approach to cross the tactile sim-to-real gap?

We implemented five different sim-to-real approaches, including the proposed approach that used tactile in the observation. In this experiment, we first compared system identification and domain randomisation approaches. Then, we examined the use of encoders to cross the sim-to-real gap.

Baseline2, Baseline4 and the proposed approach were trained on domain randomisation, while Baseline3 and Baseline5 used the calibrated tactile model during training. From the plot, the differences in success rates between simulation and reality for Baseline2 and Baseline4 are large. This implies that these two policies may have been trained on the overly large domain randomisation ranges. Among all the compared baselines, Baseline3 had the most consistent results in both environments across all objects. However, the proposed approach still performed the best. This suggests that a carefully determined domain randomisation range could still outperform a policy trained on only the calibrated tactile model.

Then, we examined the effectiveness of crossing the reality gap with encoders. Baseline4 and Baseline5 used the same encoder to encode both the simulated and real tactile signals. On the other hand, the proposed approach trained the second encoder, $\hat{S_{real}}$, to close the reality gap in the latent space. From the plot, Baseline5 performed the poorest, followed by Baseline4. We suspect the reality gap present in the simulated and real tactile signals may have been amplified by the $\hat{S_{sim}}$ in Baseline5.

According to our experiments, the proposed approach achieved the most consistent performance in both environments for all the objects. The grasping results can be seen on Fig. 5(b) and (c). We have shown that the most effective way to minimise the sim-to-real gap is to use the suitable domain randomisation ranges, with the help of additional encoders to minimise the gap in the latent space.

V. CONCLUSIONS

Our works have shown an effective way of modelling the deformable tactile sensor in simulation and learning a tactile-based policy that can be transferred to reality. We proposed to leverage a mass-spring-damper system to model each taxel of the sensor. This allows the sensor to achieve a similar deformation to the real tactile sensor in simulation when being indented. To cross the reality gap, we first leveraged an evolution strategy to estimate the parameter distributions for each taxel. The distributions were used to sample various environments during policy training with the aim to increase the robustness of the policy to different environments. Then, we further crossed the reality gap of the tactile signal in the latent space with the helps of encoders.

The paper then answered the questions raised through experiments. From the results, we have shown that the sensor model in the simulation can provide good alternatives to the reality in providing large-scale training data. Through a precision grasping task, we then realised that the tactile feedback could provide information about physical interactions essential to the robot. In our experiments, different sim-to-real strategies have been implemented to train a tactile-based grasping policy. Our tactile modelling and sim-to-real strategy have outperformed all the baselines in challenging objects. The framework presented in this paper has also been shown generalisable to other robot learning methods and other tactile sensor arrays.

REFERENCES

[1] R. S. Johansson and J. R. Flanagan, "Coding and use of tactile signals from the fingertips in object manipulation tasks," *Nature Reviews Neuroscience*, vol. 10, no. 5, pp. 345–359, 2009.

[2] R. S. Dahiya, G. Metta, M. Valle, and G. Sandini, "Tactile sensing—from humans to humanoids," *IEEE transactions on robotics*, vol. 26, no. 1, pp. 1–20, 2009.

[3] K. Wu, S. Fan, Y. Zhang, Z. Chen, H. Liu, and H. Cai, "Research of a novel miniature tactile sensor for five-finger dexterous robot hand," in *2010 IEEE International Conference on Mechatronics and Automation*. IEEE, 2010, pp. 422–427.

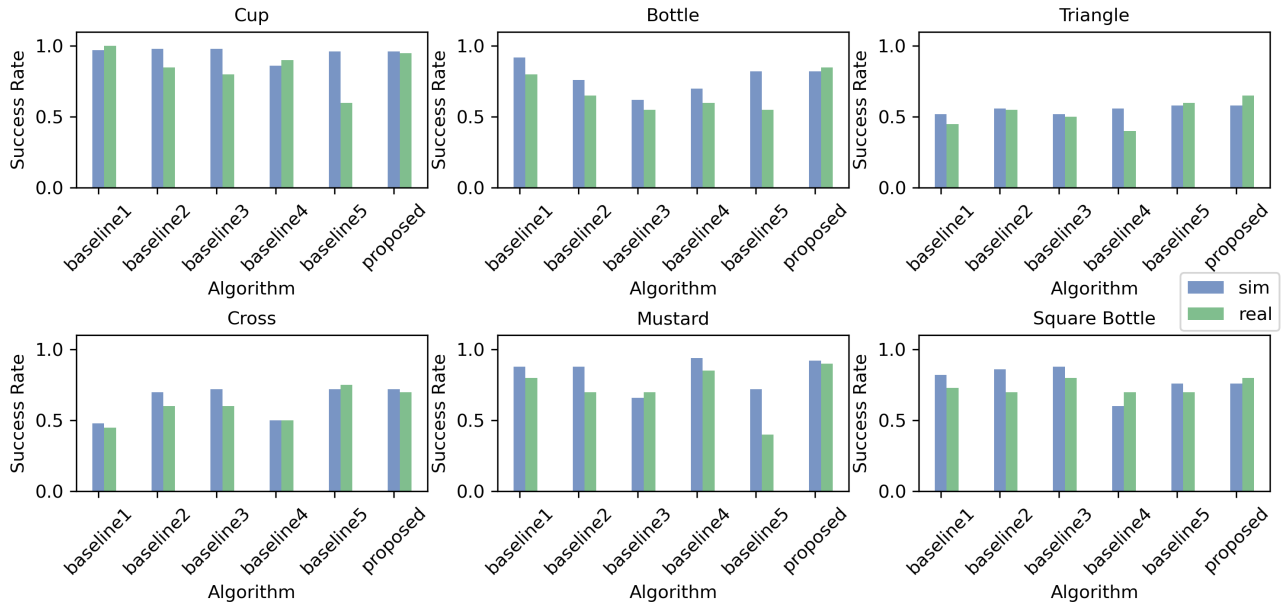

Fig. 6: Comparison of success rate in grasping between simulation and reality

[4] J. A. Jørgensen and H. G. Petersen, "Usage of simulations to plan stable grasping of unknown objects with a 3-fingered schunk hand," in *Workshop on robot simulators (IROS08)*, 2008.

[5] A. Schmitz, M. Maggiali, L. Natale, B. Bonino, and G. Metta, "A tactile sensor for the fingertips of the humanoid robot icub," in *2010 IEEE/RSJ International Conference on Intelligent Robots and Systems*. IEEE, 2010, pp. 2212–2217.

[6] Y. Wang, W. Huang, B. Fang, F. Sun, and C. Li, "Elastic tactile simulation towards tactile-visual perception," in *Proceedings of the 29th ACM International Conference on Multimedia*, 2021, pp. 2690–2698.

[7] Y. S. Narang, B. Sundaralingam, K. Van Wyk, A. Mousavian, and D. Fox, "Interpreting and predicting tactile signals for the syntouch biotac," *The International Journal of Robotics Research*, vol. 40, no. 12-14, pp. 1467–1487, 2021.

[8] D. F. Gomes, P. Paoletti, and S. Luo, "Generation of gelsight tactile images for sim2real learning," *IEEE Robotics and Automation Letters*, vol. 6, no. 2, pp. 4177–4184, 2021.

[9] H.-K. Lee, S.-I. Chang, and E. Yoon, "A flexible polymer tactile sensor: Fabrication and modular expandability for large area deployment," *Journal of microelectromechanical systems*, vol. 15, no. 6, pp. 1681–1686, 2006.

[10] A. Schmitz, P. Maiolino, M. Maggiali, L. Natale, G. Cannata, and G. Metta, "Methods and technologies for the implementation of large-scale robot tactile sensors," *IEEE Transactions on Robotics*, vol. 27, no. 3, pp. 389–400, 2011.

[11] R. Russell, "Compliant-skin tactile sensor," in *Proceedings. 1987 IEEE International Conference on Robotics and Automation*, vol. 4. IEEE, 1987, pp. 1645–1648.

[12] Z. Ding, Y.-Y. Tsai, W. W. Lee, and B. Huang, "Sim-to-real transfer for robotic manipulation with tactile sensory," in *2021 IEEE/RSJ International Conference on Intelligent Robots and Systems (IROS)*. IEEE, 2021, pp. 6778–6785.

[13] J. A. Fishel and G. E. Loeb, "Sensing tactile microvibrations with the biotac—comparison with human sensitivity," in *2012 4th IEEE RAS & EMBS international conference on biomedical robotics and biomechatronics (BioRob)*. IEEE, 2012, pp. 1122–1127.

[14] E. Donlon, S. Dong, M. Liu, J. Li, E. Adelson, and A. Rodriguez, "Gelslim: A high-resolution, compact, robust, and calibrated tactile-sensing finger," in *2018 IEEE/RSJ International Conference on Intelligent Robots and Systems (IROS)*. IEEE, 2018, pp. 1927–1934.

[15] B. Ward-Cherrier, N. Pestell, L. Cramphorn, B. Winstone, M. E. Giannaccini, J. Rossiter, and N. F. Lepora, "The tactip family: Soft optical tactile sensors with 3d-printed biomimetic morphologies," *Soft robotics*, vol. 5, no. 2, pp. 216–227, 2018.

[16] W. Yuan, S. Dong, and E. H. Adelson, "Gelsight: High-resolution robot tactile sensors for estimating geometry and force," *Sensors*, vol. 17, no. 12, p. 2762, 2017.

[17] S. L. Ricker and R. Ellis, "2-d finite-element models of tactile sensors," in *[1993] Proceedings IEEE International Conference on Robotics and Automation*. IEEE, 1993, pp. 941–947.

[18] C. Sferrazza, A. Wahlsten, C. Trueeb, and R. D'Andrea, "Ground truth force distribution for learning-based tactile sensing: A finite element approach," *IEEE Access*, vol. 7, pp. 173 438–173 449, 2019.

[19] Y. S. Narang, K. Van Wyk, A. Mousavian, and D. Fox, "Interpreting and predicting tactile signals via a physics-based and data-driven framework," *arXiv preprint arXiv:2006.03777*, 2020.

[20] Z. Si and W. Yuan, "Taxim: An example-based simulation model for gelsight tactile sensors," *IEEE Robotics and Automation Letters*, 2022.

[21] S. Wang, M. Lambeta, P.-W. Chou, and R. Calandra, "Tacto: A fast, flexible, and open-source simulator for high-resolution vision-based tactile sensors," *IEEE Robotics and Automation Letters*, vol. 7, no. 2, pp. 3930–3937, 2022.

[22] Z. Si, Z. Zhu, A. Agarwal, S. Anderson, and W. Yuan, "Grasp stability prediction with sim-to-real transfer from tactile sensing," in *2022 IEEE/RSJ International Conference on Intelligent Robots and Systems (IROS)*. IEEE, 2022, pp. 7809–7816.

[23] M. B. Villalonga, A. Rodriguez, B. Lim, E. Valls, and T. Sechopoulos, "Tactile object pose estimation from the first touch with geometric contact rendering," in *Conference on Robot Learning*. PMLR, 2021, pp. 1015–1029.

[24] S. Moisio, B. León, P. Korkealaakso, and A. Morales, "Model of tactile sensors using soft contacts and its application in robot grasping simulation," *Robotics and Autonomous Systems*, vol. 61, no. 1, pp. 1–12, 2013.

[25] J. A. Joergensen, L.-P. Ellekilde, and H. G. Petersen, "Robworksim-an open simulator for sensor based grasping," in *ISR 2010 (41st International Symposium on Robotics) and ROBOTIK 2010 (6th German Conference on Robotics)*. VDE, 2010, pp. 1–8.

[26] Z. Kappassov, J.-A. Corrales-Ramon, and V. Perdereau, "Simulation of tactile sensing arrays for physical interaction tasks," in *2020 IEEE/ASME International Conference on Advanced Intelligent Mechatronics (AIM)*. IEEE, 2020, pp. 196–201.

[27] Z. Ding, N. F. Lepora, and E. Johns, "Sim-to-real transfer for optical tactile sensing," in *2020 IEEE International Conference on Robotics and Automation (ICRA)*. IEEE, 2020, pp. 1639–1645.

[28] Y. Narang, B. Sundaralingam, M. Macklin, A. Mousavian, and D. Fox, "Sim-to-real for robotic tactile sensing via physics-based simulation and learned latent projections," in *2021 IEEE International Conference on Robotics and Automation (ICRA)*, 2021, pp. 6444–6451.

[29] A. Church, J. Lloyd, N. F. Lepora *et al.*, "Tactile sim-to-real policy transfer via real-to-sim image translation," in *Conference on Robot Learning*. PMLR, 2022, pp. 1645–1654.

[30] T. Bi, C. Sferrazza, and R. D'Andrea, "Zero-shot sim-to-real transfer of tactile control policies for aggressive swing-up manipulation," *IEEE Robotics and Automation Letters*, vol. 6, no. 3, pp. 5761–5768, 2021.

[31] C. Sferrazza and R. D'Andrea, "Sim-to-real for high-resolution optical tactile sensing: From images to 3d contact force distributions," *arXiv preprint arXiv:2012.11295*, 2020.

[32] S. Cremer, M. N. Saadatzi, I. B. Wijayasinghe, S. K. Das, M. H. Saadatzi, and D. O. Popa, "Skinsim: A design and simulation tool for robot skin with closed-loop phri controllers," *IEEE Transactions on Automation Science and Engineering*, vol. 18, no. 3, pp. 1302–1314, 2020.

[33] N. Hansen, "The cma evolution strategy: a comparing review," in *Towards a new evolutionary computation*. Springer, 2006, pp. 75–102.